HHS Public Access

Author manuscript

Cell Rep. Author manuscript; available in PMC 2019 June 27.

Published in final edited form as:

Cell Rep. 2019 February 26; 26(9): 2289–2297.e3. doi:10.1016/j.celrep.2019.01.114.

The Role of $Ca_V2.1$ Channel Facilitation in Synaptic Facilitation

Christopher Weyrer[1,2], **Josef Turecek**[1], **Zachary Niday**[1], **Pin W. Liu**[1], **Evanthia Nanou**[3], **William A. Catterall**[3], **Bruce P. Bean**[1], and **Wade G. Regehr**[1,4,*]

[1]Department of Neurobiology, Harvard Medical School, Boston, MA 02115, USA

[2]Department of Physiology, Development, and Neuroscience, University of Cambridge, Cambridge CB2 3EG, UK

[3]Department of Pharmacology, University of Washington, Seattle, WA 98195-7280, USA

[4]Lead Contact

SUMMARY

Activation of $Ca_V2.1$ voltage-gated calcium channels is facilitated by preceding calcium entry. Such self-modulatory facilitation is thought to contribute to synaptic facilitation. Using knockin mice with mutated $Ca_V2.1$ channels that do not facilitate (Ca IM-AA mice), we surprisingly found that, under conditions of physiological calcium and near-physiological temperatures, synaptic facilitation at hippocampal CA3 to CA1 synapses was not attenuated in Ca IM-AA mice and facilitation was paradoxically more prominent at two cerebellar synapses. Enhanced facilitation at these synapses is consistent with a decrease in initial calcium entry, suggested by an action-potential-evoked $Ca_V2.1$ current reduction in Purkinje cells from Ca IM-AA mice. In wild-type mice, $Ca_V2.1$ facilitation during high-frequency action potential trains was very small. Thus, for the synapses studied, facilitation of calcium entry through $Ca_V2.1$ channels makes surprisingly little contribution to synaptic facilitation under physiological conditions. Instead, $Ca_V2.1$ facilitation offsets $Ca_V2.1$ inactivation to produce remarkably stable calcium influx during high-frequency activation.

Graphical Abstract

*Correspondence: wade_regehr@hms.harvard.edu.

AUTHOR CONTRIBUTIONS C.W., J.T., B.P.B., and W.G.R. conceived the experiments. C.W. conducted experiments in Figures 1B–1D, 2, and 3. J.T. conducted experiments in Figures 1C, 1D, 2B, and 3. Z.N. conducted experiments in Figures 4 and S1. P.W.L. conducted experiments in Figure 1A. C.W., J.T., P.W.L., and B.P.B. conducted analyses. C.W. made illustrations. E.N. and W.A.C. helped with animals and the manuscript. C.W., B.P.B., and W.G.R. wrote the manuscript, with input from all authors.

DECLARATION OF INTERESTS

The authors declare no competing interests.

SUPPLEMENTAL INFORMATION

Supplemental Information can be found with this article online at https://doi.org/10.1016/j.celrep.2019.01.114.

DATA AND SOFTWARE AVAILABILITY

Data and analysis routines are available upon request to the corresponding author.

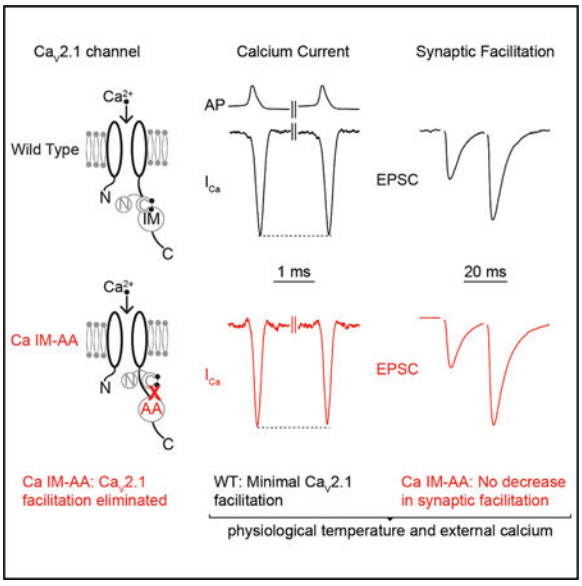

In Brief

Weyrer et al. use Ca IM-AA mice in which $Ca_V2.1$ calcium channel facilitation is eliminated to study synaptic facilitation at hippocampal and cerebellar synapses. Under conditions of physiological temperature, external calcium, and presynaptic waveforms, facilitation of $Ca_V2.1$ channels is small and does not contribute to synaptic facilitation at these synapses.

INTRODUCTION

Synaptic facilitation is a widespread form of use-dependent enhancement of neurotransmitter release that lasts for hundreds of milliseconds (Zucker and Regehr, 2002). Facilitation can counteract depression (Turecek et al., 2016, 2017), act as a temporal filter (Abbott and Regehr, 2004), is implicated in working memory (Itskov et al., 2011; Mongillo et al., 2008), and has been proposed to serve many other functional roles (Jackman and Regehr, 2017). Multiple mechanisms have been suggested to account for synaptic facilitation (Jackman and Regehr, 2017), including local saturation of calcium buffer (Blatow et al., 2003; Rozov et al., 2001), a specialized high-affinity calcium sensor such as synaptotagmin 7 (Jackman et al., 2016), and facilitation of calcium entry through voltage-gated calcium channels (Mochida et al., 2008; Nanou and Catterall, 2018; Nanou et al., 2016a).

Alterations in calcium entry have long been of special interest as a means of regulating neurotransmitter release, because at most synapses, release is highly sensitive to small changes in calcium entry (Dodge and Rahamimoff, 1967; Katz and Miledi, 1968). Typically, release varies as $(Ca_{influx})^4$ such that a 20% increase in Ca_{influx} doubles synaptic strength (Cuttle et al., 1998; Díaz-Rojas et al., 2015; Dodge and Rahamimoff, 1967; Neher and Sakaba, 2008). Most types of calcium channels exhibit calcium-dependent inactivation (Ben-Johny and Yue, 2014; Catterall and Few, 2008; Christel and Lee, 2012). However, $Ca_V2.1$ channels, which play a crucial role in transmission at many synapses, can exhibit use-dependent facilitation of calcium current (Ben-Johny and Yue, 2014; Christel and Lee,

2012; Cuttle et al., 1998; Inchauspe et al., 2004; Lee et al., 2000; Liang et al., 2003). Calmodulin (CaM) is crucially involved in $Ca_V2.1$ channel facilitation (Lee et al., 1999, 2000). CaM pre-associates with $Ca_V2.1$ channels (Erickson et al., 2001), and upon Ca^{2+} binding to its C terminus (DeMaria et al., 2001), it interacts with the IQ-like motif (IM) containing the amino acids isoleucine (I) and methionine (M) (DeMaria et al., 2001; Lee et al., 2003). Changing these amino acids to alanines (IM-AA) abolishes $Ca_V2.1$ channel facilitation (DeMaria et al., 2001; Lee et al., 2003; Zühlke et al., 2000) (Figure 1A, left).

Because of the sensitivity of transmitter release to small changes in calcium entry, it is expected that calcium-dependent facilitation of calcium entry through $Ca_V2.1$ channels should produce synaptic facilitation. Indeed, at the calyx of Held synapse (Borst and Sakmann, 1998; Cuttle et al., 1998), as well as at synapses between cultured Purkinje cells (PCs) (Díaz-Rojas et al., 2015), synaptic facilitation was accompanied by use-dependent increases in presynaptic calcium currents. The finding that calcium current facilitation was eliminated and synaptic facilitation was strongly attenuated in $Ca_V2.1$ knockout (KO) mice at the calyx of Held (Inchauspe et al., 2004; Ishikawa et al., 2005) supported a central role for $Ca_V2.1$ in synaptic facilitation. Similarly, synaptic transmission between cultured superior cervical ganglion (SCG) neurons is normally mediated by non-facilitating $Ca_V2.2$ channels, and these synapses do not facilitate (BenJohny and Yue, 2014; Liang et al., 2003; Nanou and Catterall, 2018). However, upon expression of $Ca_V2.1$ channels and subsequent blockade of $Ca_V2.2$ channels in SCG neurons, $Ca_V2.1$ channels facilitated along with synaptic transmission. In contrast, the expression of non-facilitating mutated IM-AA $Ca_V2.1$ channels led to strongly reduced facilitation of SCG synapses (Mochida et al., 2003, 2008). Ca IM-AA knockin mice, in which $Ca_V2.1$ channels are replaced by mutated IM-AA $Ca_V2.1$ channels, are a powerful tool for testing the contribution of $Ca_V2.1$ facilitation to synaptic facilitation (Nanou et al., 2016b, 2016a, 2018). Synaptic facilitation was eliminated or attenuated at some synapses in Ca IM-AA mice, suggesting that facilitation of $Ca_V2.1$ channels can account for a significant fraction of synaptic facilitation at the neuromuscular junction (NMJ), CA3 to CA1 (CA3-CA1), and CA3 to parvalbumin-expressing (PV) basket cell synapses (Nanou et al., 2016b, 2016a, 2018).

However, many factors can influence short-term synaptic plasticity, and the contribution of $Ca_V2.1$ channel facilitation to synaptic facilitation under physiological conditions of temperature and external calcium (Ca_{ext}) with calcium entry during action potential waveforms is still unclear. Quantification of facilitation of voltageclamped $Ca_V2.1$ channels has mostly been performed at room temperature, often using voltage steps lasting longer than action potentials and with relatively high Ca_{ext}. Temperature is a crucial factor, because action potential width, calcium channel activation kinetics, and kinetics of protein-protein interactions are all strongly temperature dependent. Prolonged voltage steps and high Ca_{ext} may tend to increase the extent of $Ca_V2.1$ channel facilitation. Many previous studies characterizing $Ca_V2.1$ channel facilitation in synaptic facilitation were performed in the presence of $Ca_V2.2$ antagonists to isolate effects on $Ca_V2.1$ channels. However, inhibiting calcium entry through $Ca_V2.2$ channels could potentially modify many calcium-dependent processes in presynaptic terminals and decrease the initial probability of release. In addition, at many synapses, the deletion of synaptotagmin 7 eliminates synaptic facilitation, even though this should not affect calcium channel facilitation and does not produce alterations in

presynaptic calcium signals (Jackman et al., 2016). We therefore assessed the contribution of $Ca_V2.1$ facilitation to synaptic facilitation under conditions of physiological Ca_{ext} (1.5 mM) at near-physiological temperatures and in the absence of $Ca_V2.2$ blockers. Under these conditions, we unexpectedly found that synaptic facilitation at three different synapses was not attenuated in Ca IM-AA mice. Also, under similar conditions of temperature and Ca_{ext}, wild-type (WT) $Ca_V2.1$ channel facilitation surprisingly was very small. We therefore conclude that at the synapses we tested, $Ca_V2.1$ channel facilitation makes surprisingly little contribution to synaptic facilitation under conditions of physiological Ca_{ext} and temperature and may instead serve primarily to counteract calcium channel inactivation.

RESULTS

In order to determine the role of facilitation of calcium entry in synaptic transmission, we studied knockin mice (Ca IM-AA mice) in which WT $Ca_V2.1$ calcium channels are replaced by $Ca_V2.1$ calcium channels containing an IM that has been mutated to prevent calcium-dependent facilitation of calcium entry (DeMaria et al., 2001; Lee et al., 2003; Mochida et al., 2008; Nanou et al., 2016a) (Figure 1A, left). We initially characterized the properties of calcium entry in acutely dissociated PCs using conditions similar to those used previously (30 stimuli at 100 Hz, 5-ms voltage steps at room temperature in 10 mM external Ca^{2+}). Maximal use-dependent facilitation of calcium currents of ~19% was apparent in WT mice, which was replaced by maximal use-dependent depression of ~26% in Ca IM-AA mice (Figure 1A, right; Table S1). These findings confirm that calcium-dependent facilitation of $Ca_V2.1$ calcium channels in cerebellar Purkinje neurons is eliminated in Ca IM-AA mice, as described previously for $Ca_V2.1$ channels in SCG and hippocampal neurons (Mochida et al., 2008; Nanou et al., 2016a). They also illustrate how calcium-dependent facilitation can serve to offset calcium-dependent inactivation in Cav2.1 channels in native neurons.

We then sought to determine the extent to which facilitation of calcium entry contributes to facilitation of synaptic transmission in physiological Ca_{ext} (1.5 mM) at 33°C–36°C in the absence of $Ca_V2.2$ channel antagonists. We performed experiments in the presence of $GABA_A$ receptor blockers to better isolate excitatory postsynaptic currents (EPSCs) for quantification and also in the presence of $GABA_B$ receptor blockers to avoid confounding changes in synaptic strength resulting from $GABA_B$-mediated presynaptic inhibition, especially during trains. To obtain a more complete picture of the role of $Ca_V2.1$ facilitation in synaptic facilitation, we studied three types of synapses with diverse properties. We used acute brain slices and stimulated synaptic inputs with pairs of pulses separated by different inter-stimulus intervals (ISIs) to determine paired-pulse plasticity of the postsynaptic currents (PSCs).

Contrary to the expectation that synaptic facilitation would be attenuated in Ca IM-AA mice, at hippocampal CA3-CA1 synapses, the amplitudes and decays of exponential fits were not statistically significantly different in WT and Ca IM-AA mice (Figure 1B; Table S1). Even more surprisingly, synaptic facilitation was actually enhanced in the Ca IM-AA mice at the cerebellar parallel fiber to PC (PF-PC) synapse. In WT animals, the paired-pulse ratio (PPR) peaked at 10 ms with a 2.7-fold increase and decayed with a time constant of 47 ms. In Ca IM-AA mice, the maximal mean PPR was virtually identical for short ISIs (2.8-fold at 10

ms), but facilitation was longer lived and decayed with a time constant of 85 ms. While the amplitudes of the exponential facilitation fit are not significantly different, the decay time constants are significantly different (Figure 1C; Table S1). Thus, unexpectedly, facilitation is actually larger in Ca IM-AA mice than in WT mice at PF-PC synapses for some ISIs. The results were even more surprising at the PC to deep cerebellar nuclei (PC-DCN) synapse. Short-term plasticity at this synapse is complicated and consists of a combination of facilitation and depression (Turecek et al., 2016, 2017). In 1.5 mM Ca_{ext}, the initial probability of release is sufficiently high that depression dominates the PPR in WT animals. Surprisingly, in PC-DCN synapses of Ca IM-AA mice, synaptic facilitation was prominent, whereas in WT mice, synaptic depression dominated (Figure 1D; Table S1). Thus, at all three synapses tested, two glutamatergic and one GABAergic, the maximal paired-pulse facilitation (PPF) was either the same or larger in Ca IM-AA mice in 1.5 mM Ca_{ext} at near-physiological temperatures.

Neurons often fire in bursts under physiological conditions. We therefore examined short-term plasticity during synaptic activation consisting of ten electrical pulses at different frequencies using a similar approach and experimental conditions used to study paired-pulse plasticity (Figures 2). For WT mice at hippocampal CA3-CA1 synapse, synaptic enhancement plateaued at 2- to 3-fold and the extent of synaptic enhancement was frequency dependent (Figure 2A, black; Table S1). The maximal train facilitation and frequency dependence of synaptic enhancement was unaltered in Ca IM-AA mice (Figure 2A, red; Table S1). For the PF-PC synapse in WT mice, the synaptic enhancement reached 3-fold, and the extent of synaptic enhancement was also frequency dependent (Figure 2B, black; Table S1). We found, however, that the maximal enhancement of PF-PC synapses was significantly larger in Ca IM-AA mice during trains (up to 4-fold), which is consistent with the prolonged decay of PPF in Ca IM-AA mice (Figure 1C; Table S1).

A different approach was required for the PC-DCN synapse. PCs fire spontaneously at frequencies of 10 Hz to over 100 Hz, and therefore, sustained synaptic activation is more physiologically relevant. WT PC-DCN synapses depress until they reach a steady-state amplitude (Turecek et al., 2016, 2017) (Figures 3A, 3B, and 3E, black; Table S1). At most depressing synapses, steady-state amplitudes are smaller as the frequency of activation is increased, but at PC-DCN synapses, this is not the case, and steady-state amplitudes of the PC-DCN synapse are frequency invariant over a broad range of stimulus frequencies in WT animals (Figure 3B, black). Even though depression dominates short-term plasticity during trains, the net plasticity reflects a combination of facilitation and depression, and facilitation is essential for the frequency invariance of this synapse. The elimination of facilitation is predicted to lead to a frequency-dependent synapse (Turecek et al., 2017). However, this was not the case. In Ca IM-AA mice, synaptic responses facilitated slightly at the start of stimulation and responses reached steady-state levels that were elevated relative to WT animals, but steady-state responses remained frequency invariant (Figures 3A and 3E). Facilitation can be studied more directly by stimulating with 10-Hz trains and abruptly increasing the stimulus frequency to 100 Hz (Figures 3C and 3D, black; Table S1). Facilitation was actually much more prominent in Ca IM-AA mice than in WT mice. Thus, synaptic responses evoked by stimulus trains are inconsistent with responses predicted to occur if facilitation of influx through $Ca_V2.1$ is the primary mechanism of facilitation.

The larger synaptic facilitation in Ca IM-AA mice observed at the PF-PC and PC-DCN synapses suggests that some additional aspect of transmission is altered in Ca IM-AA mice. One possible explanation is that initial calcium influx is decreased in Ca IM-AA mice. At many synapses, reducing calcium influx lowers the initial probability of release, thereby decreasing vesicle depletion and increasing synaptic facilitation (Jackman and Regehr, 2017; Zucker and Regehr, 2002). We have previously examined the properties of the PC to DCN synapse in WT animals in normal (1.5 mM) and 1.0 mM Ca_{ext} (Turecek et al., 2017). The responses measured in 1.5 mM Ca_{ext} previously and in the current study were very similar (Figure 3E). In contrast, the responses of PC-DCN synapses in Ca IM-AA mice in 1.5 mM Ca_{ext} were similar to synaptic responses measured previously in WT animals in 1.0 mM Ca_{ext} (Turecek et al., 2017) (Figure 3E). These findings suggest that a large reduction in presynaptic calcium entry could account for the synaptic responses of PC-DCN synapses in Ca IM-AA mice.

Given the large effect of the IM-AA mutation on $Ca_V2.1$ channel facilitation described previously (Nanou et al., 2016b, 2016a) and shown in Figure 1A, the observation that, in 1.5 Ca_{ext}, at 33°C–36°C, and without blocking other voltage-gated calcium channels, synaptic facilitation was not attenuated in Ca IM-AA mice (Figures 1B–1D, 2, and 3) was surprising. One possible explanation is that calcium current experiments were performed under conditions that tended to maximize facilitation of $Ca_V2.1$ channels for biophysical studies (10 mM Ca_{ext}, room temperature, and 5-ms voltage steps). In previous studies measuring presynaptic calcium levels with fluorescent indicators at 34°C in 2 mM Ca_{ext} for pairs of stimuli we did not detect significant use-dependent changes in presynaptic calcium influx for hippocampal CA3 pyramidal cells and cerebellar granule cells (Brenowitz and Regehr, 2007; Jackman et al., 2016). Measurements of changes in presynaptic calcium levels in cerebellar granule cells induced by brief trains at 34°C are consistent with small increases in calcium entry by the end of the train (Kreitzer and Regehr, 2000), but such increases could also arise from buffer saturation (Klingauf and Neher, 1997; Neher, 1998). Voltage-clamp methods can provide precise quantification of calcium entry free from such ambiguity. Previous voltage-clamp experiments indicated that the extent of facilitation of calcium entry is reduced in low Ca_{ext}, elevated temperatures, and brief depolarizations (1 mM Ca_{ext}, 32°C, 1-ms step depolarizations) (Benton and Raman, 2009; Kreiner et al., 2010). The dependence of facilitation on Ca_{ext}, temperature, and voltage steps prompted us to examine facilitation of calcium currents in physiological Ca_{ext} (1.5 mM) at 37°C with trains of action potential waveforms. Experiments were performed on the somata of acutely dissociated PCs, which have a high density of $Ca_V2.1$ channels. Although the bulk residual calcium signals in presynaptic boutons and somata differ because of their very different surface-to-volume characteristics, facilitation of calcium entry is thought to be dependent on local calcium signaling near the point of entry through calcium channels, which does not depend on residual calcium signals (Borst and Sakmann, 1998; DeMaria et al., 2001; Lee et al., 2000). Voltage commands used both narrow waveforms measured from the somata of PCs and broad waveforms measured from hippocampal pyramidal cells. These waveforms span the range of action potential shapes typical of central neurons including those recorded in presynaptic boutons (Bischofberger et al., 2002; Boudkkazi et al., 2011; Foust et al., 2011; Geiger and Jonas, 2000; Kim et al., 2010; Hoppa et al., 2014; Rowan et al., 2014), thereby

accounting for possible differences in action potential width between soma and presynaptic terminals.

We began by focusing on the initial pair of pulses during pulse trains to compare $Ca_V2.1$ facilitation with synaptic PPR (Figure 2). $Ca_V2.1$ calcium currents were isolated pharmacologically. Surprisingly, for identical action potentials (recorded from spontaneously active PCs with physiological Ca_{ext} and temperature) separated by 10 ms, there was no significant facilitation of calcium currents (I_{Ca2}/I_{Ca1}) in WT mice and little difference between WT and Ca IM-AA mice (Figure 4A; Table S1). In WT animals, 100-Hz stimulation evoked remarkably stable calcium currents, as is shown for the initial 10 stimuli of the train (Figure 4B) and summarized for the 30 stimuli (Figure 4C). The ratio of the amplitudes of the currents evoked by the 30th stimulus and first stimulus is I_{Ca30}/ I_{Ca1} = 1.01 ± 0.01 in WT animals, whereas in Ca IM-AA mice, there was a decrement in calcium entry (I_{Ca30}/I_{Ca1} = 0.95 ± 0.02). For 50-Hz stimulation, there was no significant alteration of calcium current even with sustained activation in either WT (I_{Ca30}/I_{Ca1} = 0.99 ± 0.01) or Ca IM-AA mice (I_{Ca30}/I_{Ca1} = 0.96 ± 0.02).

It is possible that the properties of the action potential waveform could influence facilitation of calcium entry. The action potentials of PCs are particularly brief. The action potential waveform used in Figures 4A–4C had a width at half-amplitude of ~0.20 ms, which is typical of Purkinje neuron action potentials at 37°C (Carter and Bean, 2009). Many other types of neurons using $Ca_V2.1$ channels to trigger synaptic release have significantly longer-lasting action potentials. We therefore also studied calcium channel facilitation using the broader waveforms recorded from hippocampal pyramidal cells, which had a width at half-amplitude of 0.92 ms (Figures 4D–4F). Experiments were again performed in PCs where $Ca_V2.1$ currents are dominant and readily isolated. As expected, the resulting calcium currents were longer lasting than those evoked by PC waveforms, but there was little difference in the properties of facilitation from those obtained when PC waveforms were used (Figures 4D–4F; Table S1). There was no facilitation of calcium entry for pairs (Figure 4D), and there were no obvious changes in calcium entry for the first 10 stimuli at 100 Hz (Figure 4E). Similar to the results with Purkinje neuron action potential waveforms (maximal facilitation of ~2%), with long trains of hippocampal neuron action potential waveforms at 100 Hz, the currents were remarkably stable in WT neurons (maximal facilitation of ~4%) but showed a maximal decrease of ~6% over the course of 30 stimuli in Ca IM-AA neurons (Figure 4F; Table S1), as if the main difference during 100-Hz trains is an unmasking of cumulative calcium current inactivation. These findings suggest that for a broad range of presynaptic waveforms, calcium entry in physiological Ca_{ext} at a physiological temperature produces little or no net facilitation of $Ca_V2.1$ currents but rather acts to compensate for cumulative inactivation, with the result being remarkable stability of calcium entry during high-frequency trains.

The synaptic properties at PF-PC synapses and PC-DCN synapses in the mutant animals are consistent with a reduction in presynaptic calcium influx. Expression levels are often altered in knockin animals, either as a result of perturbing introns or as a result of the mutations in the protein of interest. For example, disruption of Ca^{2+}/CaM binding reduces surface membrane expression of $Ca_V1.2$ channels (Wang et al., 2007). We therefore compared

calcium current densities in WT and Ca IM-AA mice. Previous studies found that the IM-AA mutation does not alter maximal current densities in cultured hippocampal neurons (Nanou et al., 2016a), which is consistent with the synaptic properties we observed at the hippocampal CA3 to CA1 synapses. However, the more pronounced increase of facilitation we observe at PF-PC and PC-DCN synapses would be consistent with small decreases in calcium entry in cerebellar granule cells and substantial decreases in PCs. We therefore quantified the magnitudes of the calcium currents evoked by 5-ms voltage steps in 1.5 mM Ca_{ext} at 37°C in PCs (Figure S1). There was a sizeable difference ($p < 0.01$) in the magnitudes of calcium currents in WT mice (1.29 ± 0.13 nA) and in Ca IM-AA mice (0.57 ± 0.05 nA), different from the situation in hippocampal neurons (Nanou et al., 2016a). Thus, in some cell types, there is a large reduction in calcium currents in Ca IM-AA mice, which would explain the observed increases in synaptic facilitation at some synapses in Ca IM-AA mice.

DISCUSSION

Our main finding is that under physiological conditions of temperature and Ca_{ext}, facilitation of native neuronal $Ca_V2.1$ channels is surprisingly small, and under similar conditions of temperature and Ca_{ext} and the absence of $Ca_V2.2$ blockers, $Ca_V2.1$ channel facilitation is clearly not the major factor underlying synaptic facilitation at CA3-CA1, PF-PC, or PC-DCN synapses.

Small Facilitation of $Ca_V2.1$ in Physiological Ca_{ext} and Temperature

We were surprised by the small facilitation of $Ca_V2.1$ currents under our conditions, because many previous studies observed much larger $Ca_V2.1$ facilitation. PPF of calcium currents mediated by $Ca_V2.1$ has been observed at the calyx of Held of (5%–20% enhancement; Borst and Sakmann, 1998; Cuttle et al., 1998; Inchauspe et al., 2004; Ishikawa et al., 2005; Müller et al., 2008), in PCs (10%; Díaz-Rojas et al., 2015), and in transfected cells (10%–35%, (DeMaria et al., 2001; Lee et al., 2000, 2003; Mochida et al., 2008). Facilitation of calcium entry has also been documented during high-frequency trains, at the calyx of Held (10%–100% enhancement; Borst and Sakmann, 1998; Cuttle et al., 1998; Muüller et al., 2008), in PCs (5%–25%; Adams et al., 2010; Benton and Raman, 2009; Chaudhuri et al., 2005), and in transfected cells (20%–35%; DeMaria et al., 2001; Lee et al., 2000, 2003; Mochida et al., 2008). However, most previous studies used non-physiological conditions that may have contributed to the large facilitation of calcium entry. In most studies, calcium currents were evoked by 1- to 10-ms repetitive voltage steps. As shown previously at the calyx of Held, larger facilitation occurs when voltage steps are used rather than action potential waveforms, most likely because such voltage steps evoke larger calcium influx (Cuttle et al., 1998; Di Guilmi et al., 2014). Similarly, many previous studies were performed in 5–10 mM Ca_{ext}, which elevates initial calcium entry and produces more facilitation of calcium influx (Chaudhuri et al., 2005). Previous studies suggest that use-dependent changes in calcium entry are much smaller when experiments are performed with brief voltage steps, in low Ca_{ext}, and at elevated temperatures (1-ms step, 1 mM Ca_{ext}, 32°C; Chaudhuri et al., 2005). Our own results highlight the strong influence of experimental conditions in regulating use-dependent changes in calcium entry. We did not observe paired-

pulse changes in calcium entry using action potential waveform stimuli with physiological conditions of temperature and Ca_{ext}, but we observed large paired-pulse increases in calcium entry in WT animals and decreases in Ca IM-AA mice (Figure 1A, right) when experiments were performed with 5-ms voltage steps at room temperature in elevated calcium.

Our results show that in physiological Ca_{ext} at physiological temperature, $Ca_V2.1$ channel facilitation is small regardless of whether a rapid PC waveform or a slow hippocampal waveform was used to evoke calcium entry. These waveforms span the range of action potential shapes typical of central neurons, including those in presynaptic boutons (Bischofberger et al., 2002; Boudkkazi et al., 2011; Foust et al., 2011; Geiger and Jonas, 2000; Kim et al., 2010; Hoppa et al., 2014; Rowan et al., 2014). Thus, our results suggest that facilitation of calcium entry is likely to be small for a broad range of presynaptic waveforms. In addition, it is actually local calcium increases near open calcium channels that facilitate entry through $Ca_V2.1$ channels (Borst and Sakmann, 1998; DeMaria et al., 2001; Lee et al., 2000). Being responsible for controlling the extent of facilitation of calcium entry, such localized calcium increases are expected to be similar for channels in the soma and in presynaptic terminals. Also, the similarity of facilitation in WT and Ca IM-AA mice at CA3 to CA1 synapses suggests that there is no facilitation of total calcium entry in the presynaptic boutons of these synapses.

Synaptic Facilitation in Physiological Ca_{ext} at Near-Physiological Temperatures

Our finding that facilitation of calcium entry does not contribute to synaptic facilitation at CA3-CA1, PF-PC, and PC-DCN synapses in physiological Ca_{ext} at near-physiological temperatures contrasts with previous demonstrations that $Ca_V2.1$ channel facilitation can contribute to the facilitation of numerous synapses under other conditions. $Ca_V2.1$ facilitation has been proposed to account for ~40% (Müller et al., 2008) or up to 100% (Inchauspe et al., 2004) of synaptic PPF at the calyx of Held synapse, up to ~100% of PPF at synapses made by cultured PCs (Díaz-Rojas et al., 2015), and up to 100% of PPF of cultured SCG synapses (Mochida et al., 2008). Previous studies in WT and Ca IM-AA mice found that calcium channel facilitation can account for up to ~60% of the maximal synaptic PPF at NMJ synapses (Nanou et al., 2016b), for close to ~100% of maximal PPF at cultured hippocampal synapses (Nanou et al., 2016a), and up to ~50% of peak PPF at hippocampal synapses in slices (Nanou et al., 2016a). However, there is no conflict between our results and previous experiments, which were performed in very different experimental conditions. These previous studies were conducted primarily at room temperature, which could have led to more prominent $Ca_V2.1$ channel facilitation than we observed at near-physiological temperatures. In addition, previous studies on facilitation at hippocampal synapses in slices (Nanou et al., 2016a, 2018) and at NMJ synapses (Nanou et al., 2016b) were performed in the presence of u-conotoxin GVIA to inhibit $Ca_V2.2$ channels. This accentuates the contribution of $Ca_V2.1$ channels to synaptic transmission at synapses such as the CA3 to CA1 synapse, where release is mediated by both $Ca_V2.1$ and $Ca_V2.2$ channels. Inhibiting $Ca_V2.2$ channels is useful for detecting effects from modification of $Ca_V2.1$ channels, but leaving the currents from $Ca_V2.2$ channels intact is preferable when using IM-AA knockin animals to quantify the effects of $Ca_V2.1$ facilitation under more physiological conditions. Our results show not only that $Ca_V2.1$ current facilitation is small for WT PCs under

physiological conditions but also that our tested synapses do not lose their prominent synaptic facilitation due to a loss of $Ca_V2.1$ current facilitation (IM-AA mutation).

Calcium Current Reduction in Ca IM-AA Mice

We found that calcium currents in PC somata were approximately half as large in Ca IM-AA mice as in WT mice, suggesting a significant decrease in channel expression. In addition, the increased synaptic facilitation and short-term plasticity at PC-DCN synapses and PF-PC synapses in Ca IM-AA mice is consistent with a reduction in presynaptic calcium entry in the presynaptic boutons of both granule cells (glutamatergic) and PCs (GABAergic). It has been established that a decrease in calcium entry increases the extent of facilitation indirectly, presumably by lowering the initial probability of release, which decreases depression associated with vesicle depletion and prevents the saturation of release (Dittman et al., 2000). However, it does not appear that $Ca_V2.1$ channel density is reduced in all types of cells, because there is no indication that calcium channel density is reduced at the CA3 to CA1 synapse, consistent with the earlier observation of no change in the amplitudes of $Ca_V2.1$ currents in cultured hippocampal neurons of Ca IM-AA animals (Nanou et al., 2016a) and our results for CA3-CA1 synapses (Figure 1B). Although the reason for the reduced $Ca_V2.1$ channel density in some cell types in Ca IM-AA mice is not known, even a small decrement in calcium channel density can strongly reduce the initial synaptic strength, which in turn increases synaptic facilitation. These results raise the possibility that changes in $Ca_V2.1$ channel density in some types of neurons could contribute to behavioral phenotypes that have been observed in Ca IM-AA mice (Nanou et al., 2016b, 2016c). We note however that a reduction in $Ca_V2.1$ current density is only one factor that may influence the balance of synaptic depression and facilitation in Ca IM-AA animals. A reduction in synaptic depression similar to that we saw in (PC-DCN) synapses is also seen in Ca IM-AA mice for the synapse of PV basket cells onto CA1 neurons (Nanou et al., 2018), in which case comparison with similar effects in calcium binding protein 1 (CaBP1) KO mice suggested mediation by altered binding of CaBP1 at the calcium sensor site. We currently have little knowledge of what calcium-binding proteins are present in presynaptic terminals of various neurons. CaBP1 does not appear to be prominent in Purkinje neurons (Kim et al., 2014) but may be involved in altered plasticity of other synapses in Ca IM-AA mice.

A Physiological Role for $Ca_V2.1$ Facilitation

In addition to self-facilitation, $Ca_V2.1$ channels also undergo both voltage-dependent and calcium-mediated inactivation. Interestingly, previous studies have shown that for native $Ca_V2.1$ channels in Purkinje neurons, cumulative inactivation is much more prominent than for $Ca_V2.1$ channels studied in heterologous transfection systems (Benton and Raman, 2009; Kreiner et al., 2010). Our own results show that in physiological Ca_{ext} at physiological temperatures, $Ca_V2.1$ facilitation in WT neurons does a remarkably good job of offsetting cumulative inactivation for the stimulation protocols commonly used to study synaptic facilitation. The resulting lack of net use-dependent changes in calcium entry in WT animals supports the hypothesis that one role of $Ca_V2.1$ facilitation is to offset inactivation to reduce the use dependence of calcium entry (Benton and Raman, 2009). In Ca IM-AA mice, 100-Hz stimulation leads to a maximal reduction in calcium entry of ~6%, which would result in a small but significant use-dependent synaptic depression of ~26%. We conclude that under

physiological conditions, $Ca_V2.1$ facilitation acts to minimize the use-dependent reduction in calcium entry that would otherwise occur and thereby minimizes a potential contribution of reduction in calcium entry to short-term plasticity. This function may be particularly valuable at synapses like the CA3-CA1 synapse, where transmission is mediated by a combination of $Ca_V2.2$ channels (showing only calcium-mediated inactivation) and $Ca_V2.1$ channels (with both inactivation and facilitation).

STAR★METHODS

CONTACT FOR REAGENT AND RESOURCE SHARING

Further information and requests should be directed to and will be fulfilled by the lead contact, Wade G. Regehr (wade_regehr@hms.harvard.edu).

EXPERIMENTAL MODEL AND SUBJECT DETAILS

Mice—Animal procedures have been carried out in accordance with the NIH guidelines and protocols were approved by the Harvard Medical Area Standing Committee on Animals. Ca IM-AA mice in which isoleucine and methionine of the $Ca_V2.1$ channel IM motif have been mutated to alanines were originally generated by ‘‘Ingenious Targeting Laboratory’’ (Nanou et al., 2016b, 2016a) and was transferred from the William Catterall laboratory at the University of Washington to Harvard Medical School. WT controls were derived from the same Ca IM-AA mouse line. Mice of either sex were used. Experimenters were blinded to the genotype of the mouse for all experiments.

METHOD DETAILS

Preparation of dissociated Purkinje neurons—Mice were deeply anesthetized with isoflurane and killed by decapitation. The cerebellum was quickly removed and placed into ice-cold solution consisting of 110 mM NaCl, 2.5 mM KCl, 10 mM HEPES, 25 mM glucose, 75 mM sucrose, 7.5 mM $MgCl_2$, pH adjusted to 7.4 with NaOH. The cerebellum was cut into (~1 mm^3) chunks and was treated for 10–20 min at room temperature with 3 mg/mL protease XXIII (Sigma Life Science) dissolved in a dissociation solution consisting of 82 mM Na_2SO_4, 30 mM K_2SO_4, 5 mM $MgCl_2$, 10 mM glucose, and 10 mM HEPES, pH adjusted to 7.4 with NaOH. The protease solution was then replaced by ice-cold dissociation solution containing 1 mg/mL trypsin inhibitor and 1 mg/mL bovine serum albumin and the chunks were kept on ice in this solution until immediately before use. To release individual cells, the tissue was passed through Pasteur pipettes with fire-polished tips. A drop of the suspension was placed in the recording chamber and diluted with a large volume of Tyrode’s solution, consisting of 155 mM NaCl, 3.5 mM KCl, 1.5 mM $CaCl_2$, 1 mM $MgCl_2$, 10 mM glucose, 10 mM HEPES, pH adjusted to 7.4 with approximately 5 mM NaOH. Purkinje neurons could be recognized by their large size and a single large dendritic stump. The used age range was P16-P19 for Figure 1A, P15-P17 for Figure 4 and P11-P17 for the current size comparisons.

Electrophysiology of dissociated Purkinje neurons—P-type calcium current in dissociated Purkinje neurons: Whole-cell patch-clamp recordings were obtained with a Multiclamp 700B amplifier (Molecular Devices), and Digidata 1322A A/D converter

(Molecular Devices), and Clampex 10.3.1.5 software (Molecular Devices). Data were analyzed using Igor-Pro 6.12A (Wavemetrics) using DataAccess (Bruxton) to read Clampex files and using Microsoft Excel. Recordings were made with borosilicate glass electrodes (VWR International) wrapped with Parafilm to reduce pipette capacitance. Pipette resistances were 1.2–3.0 MU when filled with the internal solution containing (in mM) 139.5 K-methanesulfonate, 5 tetraethylammonium (TEA) Cl, 10 NaCl, 2 $MgCl_2$, 1 EGTA, 0.2 $CaCl_2$, 4 MgATP, 0.3 GTP (Tris salt), 14 creatine phosphate (Tris salt), and 10 HEPES with pH adjusted to 7.35 with KOH. Series resistance (typically 3–6 MU) was compensated during voltage-clamp recording by 70% and monitored throughout the experiment. Voltages are corrected for a liquid junction potential of —8 mV between the internal solution and the external Tyrode's solution in which membrane current was zeroed before the start of the experiment. After a gigaohm seal, whole-cell configuration was established, the cell was lifted off the bottom of the recording chamber and placed in front of an array of quartz fiber flow pipes (250 mm internal diameter, 350 mm external diameter) glued onto an aluminum rod whose temperature was controlled by resistive heating elements and a feedback-controlled temperature controller (TC-344B, Warner Instruments). Solutions were changed (in ~1 s) by moving the cell from one pipe to another. Initial voltage clamp recordings to assay calcium current facilitation were performed at room temperature using an external solution of 10 mM $CaCl_2$, 155 mM TEACl, 10 mM HEPES, pH adjusted to 7.4 with TEA-OH. In order to isolate P-type ($Ca_V2.1$) current, the solution contained inhibitors for L-type, N-type, and T-type current (2 mM nimodipine, 1 mM conotoxin GVIA, and 1 mM TTA-A2) along with 1 mM tetrodotoxin (TTX) to inhibit outward currents through sodium channels. For recording P-type current flowing during action potential waveforms at physiological temperatures and with physiological calcium concentrations, the external solution contained 1.5 mM $CaCl_2$, 1 mM $MgCl_2$, 155 mM TEACl, 20 mM glucose, 10 HEPES, pH adjusted to 7.4 with TEA-OH, with 1 mM TTX, 2 mM nimodipine, 1 mM conotoxin GVIA, and 1 mM TTA-A2. The process of dialyzing cells to make whole-cell recordings did not disrupt calcium current facilitation, because it was robust and showed no tendency to run down in the experiments using 10 mM Ca^{2+} at room temperature with voltage steps. Recordings of action potential-evoked calcium currents were made at 37°C.

Action potential waveforms were previously recorded at 37°C in acutely dissociated CA1 pyramidal neurons and Purkinje cells using an intracellular solution containing 139.5 mM K-methanesulfonate, 10 mM NaCl, 2 mM $MgCl_2$, 1 mM EGTA, 0.2 mM $CaCl_2$, 4 mM MgATP, 0.3 mM GTP (Tris salt), 14 mM creatine phosphate (Tris salt), 10 mM HEPES, pH adjusted to 7.35 with KOH, and an external Tyrode's solution containing 155 mM NaCl, 3.5 mM KCl, 1.5 mM $CaCl_2$, 1 mM $MgCl_2$, 10 mM glucose and 10 mM HEPES with pH adjusted to 7.4 with NaOH.

In the voltage clamp recordings of P-type current, capacity currents were reduced during recording using the amplifier circuitry. In the voltage clamp experiments using step depolarizations, remaining capacity currents along with leak currents were corrected during analysis using the current evoked by a 5 mV hyperpolarization to define remaining capacity currents and leak current, which was assumed to be ohmic. For action potential waveforms, capacity and leak currents were corrected by recording the response to the action potential waveform inverted and scaled down by a factor of 4, and signal-averaging over 4

applications of this waveform. However, this correction was imperfect, particularly for the fast-rising and fast-falling Purkinje cell action potential waveforms. Therefore, to better isolate calcium current free from contaminating capacity current artifacts, after recording the P-type currents, we repeated the stimulation in a calcium-free solution, containing 5 mM $MgCl_2$, 155 mM TEACl, 20 mM glucose and 10 mM HEPES with pH adjusted to 7.4 with TEA-OH. Calcium currents were determined by subtracting the currents in Ca-free solutions from those in the Ca-containing solutions. $Sweep_2/Sweep_1$ in Figures 4A and 4D was created using the first 2 points from stimulus trains.

Preparation of acute brain slices—Mice were anesthetized with isoflurane and decapitated. A Leica VT1200S vibratome was used to cut acute slices with a thickness ranging from 250 to 270 mm. For CA3-CA1 and PF-PC recordings, slices were prepared using ice-cold choline-based oxygenated (95% O2, 5% CO2) cutting solution containing (in mM): 110 Choline-Cl, 7 $MgSO_4$ or $MgCl_2$, 2.5 KCl, 1.2 NaH_2PO_4, 0.5 $CaCl_2$, 25 glucose, 11.6 Na-Ascorbate, 2.4 Na-Pyruvate and 25 $NaHCO_3$. Transverse hippocampal and cerebellar slices were cut for CA3-CA1 and PF-PC recordings. A subset of hippocampal slices were prepared using a Leica VT1000S vibratome and ice-cold oxygenated (95% O_2, 5% CO_2) sucrose-based cutting solution containing (in mM): 234 sucrose, 25 $NaHCO_3$, 11 glucose, 7 $MgCl_2$, 2.5 KCl, 1.25 NaH_2PO_4 and 0.5 $CaCl_2$. A cut was made between the CA3 and CA1 regions of the hippocampal slices when they were still cold. Antagonists were not included in the external solution of the holding chamber. Slices for PC-DCN recordings were prepared as previously described (Turecek et al., 2016, 2017). Choline-Cl slicing solution as described above was supplemented with (in mM) 5 CPP, 5 NBQX and warmed to 35°C to make parasagittal slices.

Acute brain slices were transferred to a holding chamber and incubated at ~32–34°C for 20–30 min in oxygenated (95% O_2, 5% CO_2) artificial cerebrospinal fluid (ACSF) containing (in mM): 125 NaCl, 26 $NaHCO_3$, 1.25 NaH_2PO_4, 2.5 KCl, 25 glucose, 1.5 $CaCl_2$ and 1 $MgCl_2$. After incubation, brain slices were kept at room temperature (RT) until they were transferred individually to a recording chamber.

Electrophysiology of acute brain slices—Brain slices were transferred/mounted onto poly-L-lysine coated coverslips and/or via harp and submerged in oxygenated ACSF. The composition of the ACSF was as described above unless otherwise noted. Whole-cell voltage-clamp recordings were performed at 33–36°C. For all experiments, series resistance was compensated up to 80% and ISIs were randomized.

CA3-CA1 recordings were performed similar to (Jackman et al., 2016). P25–31 (PPR) and P25–32 (trains) animals were used. ACSF was supplemented with (in mM): 100 picrotoxin, 2 CPP and 2 CGP-55845. CA1 neurons were held at —60 mV. Borosilicate recording electrodes were filled with (in mM): 100 CsCl, 75 CsFl, 10 EGTA, 10 HEPES and 5 QX-314-Cl. For electrical stimulation a glass monopolar pipette was filled with ACSF and placed in the stratum radiatum. Initial EPSC sizes were kept at 50 to 250 pA.

For PF-PC recordings, ACSF was supplemented with (in mM): 100 picrotoxin or 1.25 gabazine, 2 CGP 55845 and 1 AM-251 (for trains only). P18–22 (PPR) and P19–22 (trains)

animals were used. Purkinje cells were held at —60 mV. Recording electrodes contained the same internal solution as for CA3-CA1 recordings. Stimulation was performed within the inner third of the molecular layer and avoided the ascending branch of parallel fibers. EPSC1 sizes were between 50 and 250 pA in order to maintain voltage clamp.

PC-DCN recordings were performed as previously described (Turecek et al., 2016, 2017). P22–32 animals were used. ACSF was supplemented with (in mM): 5 NBQX, 2 CPP, 0.5 strychnine. DCN neurons were held at —30 to —40 mV. Recording electrodes were filled with (in mM): 110 CsCl, 10 HEPES, 10 TEA-Cl, 1 $MgCl_2$, 4 $CaCl_2$, 5 EGTA, 20 Cs-BAPTA, 2 QX314, 0.2 D600. A glass monopolar stimulus electrode was placed in the white matter surrounding the DCN, as previously described. Trains of various frequencies were applied with 100 stimuli, followed by 100 stimuli at 100Hz.

Synaptic recordings were collected at 10 −20 kHz and filtered at 2 −10 kHz using an Axon Multiclamp 700B and digitized with an ITC-18 using mafPC (courtesy of Matthew A. Xu-Friedman) and custom procedures (courtesy of Skyler L. Jackman) in IgorPro (Wavemetrics). Data analysis was performed using custom scripts written in IgorPro (mainly courtesy of Skyler L. Jackman), Microsoft Excel and MATLAB (Mathworks), available upon request. For presented data, stimulus artifacts were blanked for clarity.

EPSC/IPSC amplitude was measured from averaged trials as the peak current with baseline collected just prior to the stimulus onset. During high frequency stimulation or when ISIs were small, EPSC/IPSCs did not fully decay between stimuli. For trains the baseline was measured by extrapolating a single exponential fit to the previous EPSC/IPSC. For PPR, for short ISIs the amplitude of EPSC2 was determined by subtracting EPSC1 collected for long ISI trials. For PC-DCN recordings, a subset of paired-pulse ratios was collected from train data (40 and 50 ms ISIs were pooled). PC-DCN steady-state values were measured as the average of the 50–70th IPSC size.

PPR curves for CA3-CA1 and PF-PC synapses were fit with a single exponential of the form: $\left(1 + Ae^{-(t - t0)/\tau}\right)$, with t_0 as the interstimulus interval leading to maximal PPR. PPR curves for PC-DCN synapses were more complicated and were poorly fit by a single exponential, and therefore only the peak PPR was compared. Train data for CA3-CA1 and PF-PC synapses was fit with a single exponential fit of the form $\left((1 + A) - Ae^{-(t - \tau)}\right)$.

QUANTIFICATION AND STATISTICAL ANALYSIS

The number of experiments are shown in Table S1 as number of cells (n) and number of animals (N). Fit coefficients are shown ± standard deviation (SD), and all other measurements are presented as mean ± SEM. Statistics were performed using Graphpad Prism, Microsoft Excel, Igor Pro and custom written scripts in MATLAB. Statistical tests are indicated in Table S1. Comparisons were performed using unpaired two-tailed Student's t test unless otherwise noted (see Table S1) and set with significance level of $p < 0.05$ (*). Same standard deviation was assumed for both tested populations. Single exponential fits to PPR and synaptic train data were compared using permutation tests, as described previously (Turecek and Regehr, 2018). Briefly, wild-type and Ca IM-AA data were randomly assigned

to two groups. Each group was averaged and fit with $\mathrm{PRR} = \left(1 + Ae^{-(t - t0)/\tau}\right)$ or $\mathrm{EPSC}_{\mathrm{train}} = \left((1 + A) - Ae^{-(t - \tau)}\right)$. The differences between fit coefficients of the two groups (residuals, $\mathrm{A}_1 - \mathrm{A}_2; \tau_1 - \tau_2$) were taken. 10000 repetitions were performed to generate a distribution of residuals. The observed difference between wild-type and Ca-IMAA fit coefficients was then compared to the generated distribution of residuals. P values were obtained as the number of generated residuals greater than the observed difference, with significance set to $p < 0.05$.

Supplementary Material

Refer to Web version on PubMed Central for supplementary material.

ACKNOWLEDGMENTS

We thank Skyler L. Jackman, Sandrine Pouvreau, and Kimberly McDaniels for help during the project, as well as the entire animal care staff and all current and former members of the Regehr and Bean labs who helped with this project. This work was supported by the NIH (grant R35 NS097284 to W.G.R., grant R01 NS036855 to B.P.B., and grant R01 NS022625 to W.A.C.), a Boehringer Ingelheim Fonds PhD Fellowship, a B&C Privatstiftung Forschungsfö r-derung, an Alice and Joseph Brooks Postdoctoral Fellowship (to C.W.), and a Harvard Mahoney Neuroscience Institute Postdoctoral Fellowship (to Z.N.).

REFERENCES

Abbott LF, and Regehr WG (2004). Synaptic computation. Nature 431, 796–803. [PubMed: 15483601]

Adams PJ, Rungta RL, Garcia E, van den Maagdenberg AMJM, Mac-Vicar BA, and Snutch TP (2010). Contribution of calcium-dependent facilitation to synaptic plasticity revealed by migraine mutations in the P/Q-type calcium channel. Proc. Natl. Acad. Sci. USA 107, 18694–18699. [PubMed: 20937883]

Ben-Johny M, and Yue DT (2014). Calmodulin regulation (calmodulation) of voltage-gated calcium channels. J. Gen. Physiol 143, 679–692. [PubMed: 24863929]

Benton MD, and Raman IM (2009). Stabilization of Ca current in Purkinje neurons during high-frequency firing by a balance of Ca-dependent facilitation and inactivation. Channels (Austin) 3, 393–401. [PubMed: 19806011]

Bischofberger J, Geiger JRP, and Jonas P (2002). Timing and efficacy of Ca^{2+} channel activation in hippocampal mossy fiber boutons. J. Neurosci 22, 10593–10602. [PubMed: 12486151]

Blatow M, Caputi A, Burnashev N, Monyer H, and Rozov A (2003). Ca^{2+} buffer saturation underlies paired pulse facilitation in calbindin-D28k-containing terminals. Neuron 38, 79–88. [PubMed: 12691666]

Borst JGG, and Sakmann B (1998). Facilitation of presynaptic calcium currents in the rat brainstem. J. Physiol 513, 149–155. [PubMed: 9782166]

Boudkkazi S, Fronzaroli-Molinieres L, and Debanne D (2011). Presynaptic action potential waveform determines cortical synaptic latency. J. Physiol 589, 1117–1131. [PubMed: 21224227]

Brenowitz SD, and Regehr WG (2007). Reliability and heterogeneity of calcium signaling at single presynaptic boutons of cerebellar granule cells. J. Neurosci 27, 7888–7898. [PubMed: 17652580]

Carter BC, and Bean BP (2009). Sodium entry during action potentials of mammalian neurons: incomplete inactivation and reduced metabolic efficiency in fast-spiking neurons. Neuron 64, 898–909. [PubMed: 20064395]

Catterall WA, and Few AP (2008). Calcium channel regulation and presynaptic plasticity. Neuron 59, 882–901. [PubMed: 18817729]

Chaudhuri D, Alseikhan BA, Chang SY, Soong TW, and Yue DT (2005). Developmental activation of calmodulin-dependent facilitation of cerebellar P-type Ca^{2+} current. J. Neurosci 25, 8282–8294. [PubMed: 16148236]

Christel C, and Lee A (2012). Ca^{2+}-dependent modulation of voltage-gated Ca^{2+} channels. Biochim. Biophys. Acta 1820, 1243–1252. [PubMed: 22223119]

Cuttle MF, Tsujimoto T, Forsythe ID, and Takahashi T (1998). Facilitation of the presynaptic calcium current at an auditory synapse in rat brainstem. J. Physiol 512, 723–729. [PubMed: 9769416]

DeMaria CD, Soong TW, Alseikhan BA, Alvania RS, and Yue DT (2001). Calmodulin bifurcates the local Ca^{2+} signal that modulates P/Q-type Ca^{2+} channels. Nature 411, 484–489. [PubMed: 11373682]

Di Guilmi MN, Wang T, Inchauspe CG, Forsythe ID, Ferrari MD, van den Maagdenberg AMJM, Borst JGG, and Uchitel OD (2014). Synaptic gain-of-function effects of mutant Cav2.1 channels in a mouse model of familial hemiplegic migraine are due to increased basal [Ca2+]i. J. Neurosci 34, 7047–7058. [PubMed: 24849341]

Díaz-Rojas F, Sakaba T, and Kawaguchi SY (2015). Ca($^{2+}$) current facilitation determines short-term facilitation at inhibitory synapses between cerebellar Purkinje cells. J. Physiol 593, 4889–4904. [PubMed: 26337248]

Dittman JS, Kreitzer AC, and Regehr WG (2000). Interplay between facilitation, depression, and residual calcium at three presynaptic terminals. J. Neurosci 20, 1374–1385. [PubMed: 10662828]

Dodge FA Jr., and Rahamimoff R (1967). Co-operative action a calcium ions in transmitter release at the neuromuscular junction. J. Physiol 193, 419–432. [PubMed: 6065887]

Erickson MG, Alseikhan BA, Peterson BZ, and Yue DT (2001). Preassociation of calmodulin with voltage-gated Ca($^{2+}$) channels revealed by FRET in single living cells. Neuron 31, 973–985. [PubMed: 11580897]

Foust AJ, Yu Y, Popovic M, Zecevic D, and McCormick DA (2011). Somatic membrane potential and Kv1 channels control spike repolarization in cortical axon collaterals and presynaptic boutons. J. Neurosci 31, 15490–15498. [PubMed: 22031895]

Geiger JRP, and Jonas P (2000). Dynamic control of presynaptic Ca($^{2+}$) inflow by fast-inactivating K(+) channels in hippocampal mossy fiber boutons. Neuron 28, 927–939. [PubMed: 11163277]

Hoppa MB, Gouzer G, Armbruster M, and Ryan TA (2014). Control and plasticity of the presynaptic action potential waveform at small CNS nerve terminals. Neuron 84, 778–789. [PubMed: 25447742]

Inchauspe CG, Martini FJ, Forsythe ID, and Uchitel OD (2004). Functional compensation of P/Q by N-type channels blocks short-term plasticity at the calyx of Held presynaptic terminal. J. Neurosci 24, 10379–10383. [PubMed: 15548652]

Ishikawa T, Kaneko M, Shin HS, and Takahashi T (2005). Presynaptic N-type and P/Q-type Ca^{2+} channels mediating synaptic transmission at the calyx of Held of mice. J. Physiol 568, 199–209. [PubMed: 16037093]

Itskov V, Hansel D, and Tsodyks M (2011). Short-term facilitation may stabilize parametric working memory trace. Front. Comput. Neurosci 5, 40. [PubMed: 22028690]

Jackman SL, and Regehr WG (2017). The mechanisms and functions of synaptic facilitation. Neuron 94, 447–464. [PubMed: 28472650]

Jackman SL, Turecek J, Belinsky JE, and Regehr WG (2016). The calcium sensor synaptotagmin 7 is required for synaptic facilitation. Nature 529, 88–91. [PubMed: 26738595]

Katz B, and Miledi R (1968). The role of calcium in neuromuscular facilitation. J. Physiol 195, 481–492. [PubMed: 4296699]

Kim JH, Kushmerick C, and von Gersdorff H (2010). Presynaptic resurgent Na^{+} currents sculpt the action potential waveform and increase firing reliability at a CNS nerve terminal. J. Neurosci 30, 15479–15490. [PubMed: 21084604]

Kim KY, Scholl ES, Liu X, Shepherd A, Haeseleer F, and Lee A (2014). Localization and expression of CaBP1/caldendrin in the mouse brain. Neuroscience 268, 33–47. [PubMed: 24631676]

Klingauf J, and Neher E (1997). Modeling buffered Ca^{2+} diffusion near the membrane: implications for secretion in neuroendocrine cells. Biophys. J 72, 674–690. [PubMed: 9017195]

Kreiner L, Christel CJ, Benveniste M, Schwaller B, and Lee A (2010). Compensatory regulation of Cav2.1 Ca^{2+} channels in cerebellar Purkinje neurons lacking parvalbumin and calbindin D-28k. J. Neurophysiol 103, 371–381. [PubMed: 19906882]

Kreitzer AC, and Regehr WG (2000). Modulation of transmission during trains at a cerebellar synapse. J. Neurosci 20, 1348–1357. [PubMed: 10662825]

Lee A, Wong ST, Gallagher D, Li B, Storm DR, Scheuer T, and Catterall WA (1999). Ca^{2+}/calmodulin binds to and modulates P/Q-type calcium channels. Nature 399, 155–159. [PubMed: 10335845]

Lee A, Scheuer T, and Catterall WA (2000). Ca^{2+}/calmodulin-dependent facilitation and inactivation of P/Q-type Ca^{2+} channels. J. Neurosci 20, 6830–6838. [PubMed: 10995827]

Lee A, Zhou H, Scheuer T, and Catterall WA (2003). Molecular determinants of Ca($^{2+}$)/calmodulin-dependent regulation of Ca(v)2.1 channels. Proc. Natl. Acad. Sci. USA 100, 16059–16064. [PubMed: 14673106]

Liang H, DeMaria CD, Erickson MG, Mori MX, Alseikhan BA, and Yue DT (2003). Unified mechanisms of Ca^{2+} regulation across the Ca2+ channel family. Neuron 39, 951–960. [PubMed: 12971895]

Mochida S, Westenbroek RE, Yokoyama CT, Itoh K, and Catterall WA (2003). Subtype-selective reconstitution of synaptic transmission in sympathetic ganglion neurons by expression of exogenous calcium channels. Proc. Natl. Acad. Sci. USA 100, 2813–2818. [PubMed: 12601155]

Mochida S, Few AP, Scheuer T, and Catterall WA (2008). Regulation of presynaptic Ca(V)2.1 channels by Ca^{2+} sensor proteins mediates short-term synaptic plasticity. Neuron 57, 210–216. [PubMed: 18215619]

Mongillo G, Barak O, and Tsodyks M (2008). Synaptic theory of working memory. Science 319, 1543–1546. [PubMed: 18339943]

Müller M, Felmy F, and Schneggenburger R (2008). A limited contribution of Ca^{2+} current facilitation to paired-pulse facilitation of transmitter release at the rat calyx of Held. J. Physiol 586, 5503–5520. [PubMed: 18832426]

Nanou E, and Catterall WA (2018). Calcium channels, synaptic plasticity, and neuropsychiatric disease. Neuron 98, 466–481. [PubMed: 29723500]

Nanou E, Sullivan JM, Scheuer T, and Catterall WA (2016a). Calcium sensor regulation of the $Ca_V2.1$ Ca^{2+} channel contributes to short-term synaptic plasticity in hippocampal neurons. Proc. Natl. Acad. Sci. USA 113, 1062–1067. [PubMed: 26755594]

Nanou E, Yan J, Whitehead NP, Kim MJ, Froehner SC, Scheuer T, and Catterall WA (2016b). Altered short-term synaptic plasticity and reduced muscle strength in mice with impaired regulation of presynaptic CaV2.1 Ca^{2+} channels. Proc. Natl. Acad. Sci. USA 113, 1068–1073. [PubMed: 26755585]

Nanou E, Scheuer T, and Catterall WA (2016c). Calcium sensor regulation of the CaV2.1 Ca^{2+} channel contributes to long-term potentiation and spatial learning. Proc. Natl. Acad. Sci. USA 113, 13209–13214. [PubMed: 27799552]

Nanou E, Lee A, and Catterall WA (2018). Control of excitation/inhibition balance in a hippocampal circuit by calcium sensor protein regulation of presynaptic calcium channels. J. Neurosci 38, 4430–4440. [PubMed: 29654190]

Neher E (1998). Usefulness and limitations of linear approximations to the understanding of Ca++ signals. Cell Calcium 24, 345–357. [PubMed: 10091004]

Neher E, and Sakaba T (2008). Multiple roles of calcium ions in the regulation of neurotransmitter release. Neuron 59, 861–872. [PubMed: 18817727]

Rowan MJM, Tranquil E, and Christie JM (2014). Distinct Kv channel sub-types contribute to differences in spike signaling properties in the axon initial segment and presynaptic boutons of cerebellar interneurons. J. Neurosci 34, 6611–6623. [PubMed: 24806686]

Rozov A, Burnashev N, Sakmann B, and Neher E (2001). Transmitter release modulation by intracellular Ca^{2+} buffers in facilitating and depressing nerve terminals of pyramidal cells in layer 2/3 of the rat neocortex indicates a target cell-specific difference in presynaptic calcium dynamics. J. Physiol 531, 807–826. [PubMed: 11251060]

Turecek J, and Regehr WG (2018). Synaptotagmin 7 mediates both facilitation and asynchronous release at granule cell synapses. J. Neurosci 38, 3240–3251. [PubMed: 29593071]

Turecek J, Jackman SL, and Regehr WG (2016). Synaptic specializations support frequency-independent Purkinje Cell output from the cerebellar cortex. Cell Rep 17, 3256–3268. [PubMed: 28009294]

Turecek J, Jackman SL, and Regehr WG (2017). Synaptotagmin 7 confers frequency invariance onto specialized depressing synapses. Nature 551, 503–506. [PubMed: 29088700]

Wang H-G, George MS, Kim J, Wang C, and Pitt GS (2007). Ca2+/ calmodulin regulates trafficking of Ca(V)1.2 Ca^{2+} channels in cultured hippo-campal neurons. J. Neurosci 27, 9086–9093. [PubMed: 17715345]

Zucker RS, and Regehr WG (2002). Short-term synaptic plasticity. Annu. Rev. Physiol 64, 355–405. [PubMed: 11826273]

Zühlke RD, Pitt GS, Tsien RW, and Reuter H (2000). Ca^{2+}-sensitive inactivation and facilitation of L-type Ca^{2+} channels both depend on specific amino acid residues in a consensus calmodulin-binding motif in the(a)1C subunit. J. Biol. Chem 275, 21121–21129. [PubMed: 10779517]

Highlights

- $Ca_V2.1$ facilitation did not contribute to synaptic facilitation with physiological stimuli
- $Ca_V2.1$ facilitation is small for action potentials and 1.5 mM external Ca at 37°C
- The magnitude of $Ca_V2.1$ currents can be reduced in some cell types in Ca IM-AA mice
- $Ca_V2.1$ facilitation offsets inactivation to maintain constant calcium entry

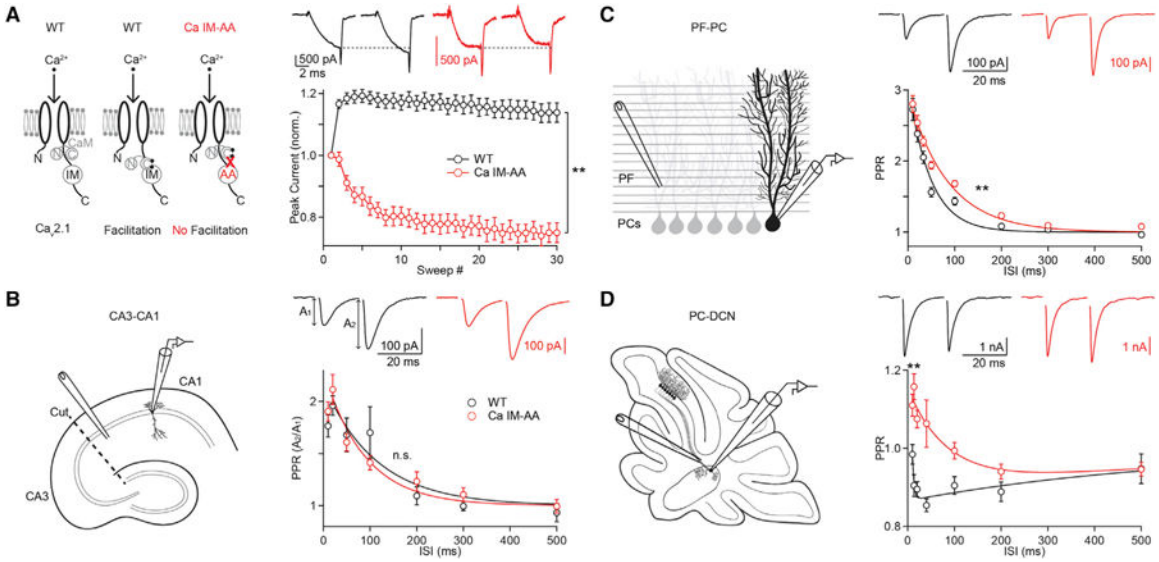

Figure 1. Paired-Pulse Synaptic Facilitation Does Not Decrease in the Absence of Ca$_V$2.1 Channel Facilitation

(A) Left: schematic of Ca$_V$2.1 channel facilitation (IM, IQ-like motif, CaM, calmodulin). Right: use-dependent facilitation of Ca$_V$2.1 current is eliminated in Ca IM-AA mice. Top: voltage steps and resulting calcium currents in dissociated PCs from WT (black) and Ca IM-AA (red) mice. Bottom: average responses (normalized to current evoked by first stimulus) plotted versus the number of sweeps for 5-ms voltage steps at 100 Hz. Calcium current experiments were performed in 10 mM Ca_{ext} at room temperature.

(B–D) Synaptic experiments were performed on wild-type (WT; black) and Ca IM-AA (red) mice at (B) the hippocampal CA3 to CA1 (CA3-CA1) synapse, (C) the cerebellar parallel fiber to PC (PF-PC) synapse, and (D) the cerebellar PC to deep cerebellar nuclei synapse (PC-DCN). Synaptic experiments were performed in mM Ca_{ext} at near-physiological temperatures. Left: schematics show the experimental configurations in which synaptic inputs were stimulated twice with an extracellular electrode and synaptic currents were recorded in whole-cell voltage clamp. Top right: representative EPSCs with an inter-stimulus interval (ISI) of 20 ms are shown for WT (black) and Ca IM-AA (red) mice. Bottom right: average paired-pulse ratio (PPR = A_1/A_2) is plotted as a function of ISI.

Statistical significance (unpaired Student's t test or permutation test; see Table S1): **p < 0.01; not significant (n.s.). Data are shown as mean ± SEM.

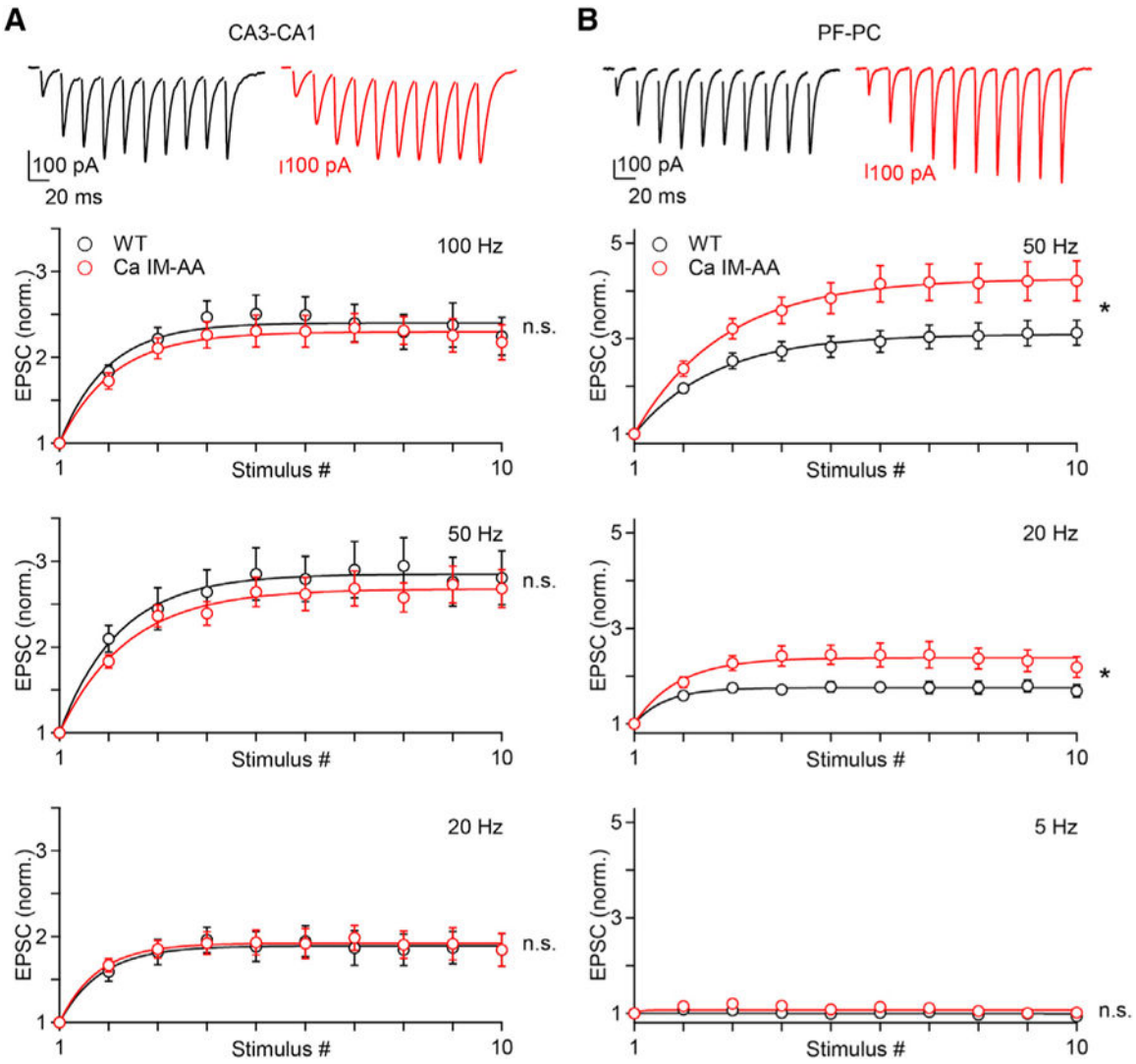

Figure 2. Synaptic Train Facilitation Does Not Decrease in Ca IM-AA Mice

(A and B) Experiments were performed in wild-type (WT; black) and Ca IM-AA (red) mice at hippocampal CA3-CA1 synapses (A) and cerebellar PF-PC synapses (B). Top: representative EPSCs evoked by a 50-Hz train. Middle and bottom: summary of normalized average EPSC amplitudes for the indicated stimulus frequencies. Statistical significance (permutation test; see Table S1): *$p < 0.05$; not significant (n.s.). Data are shown as mean ± SEM.

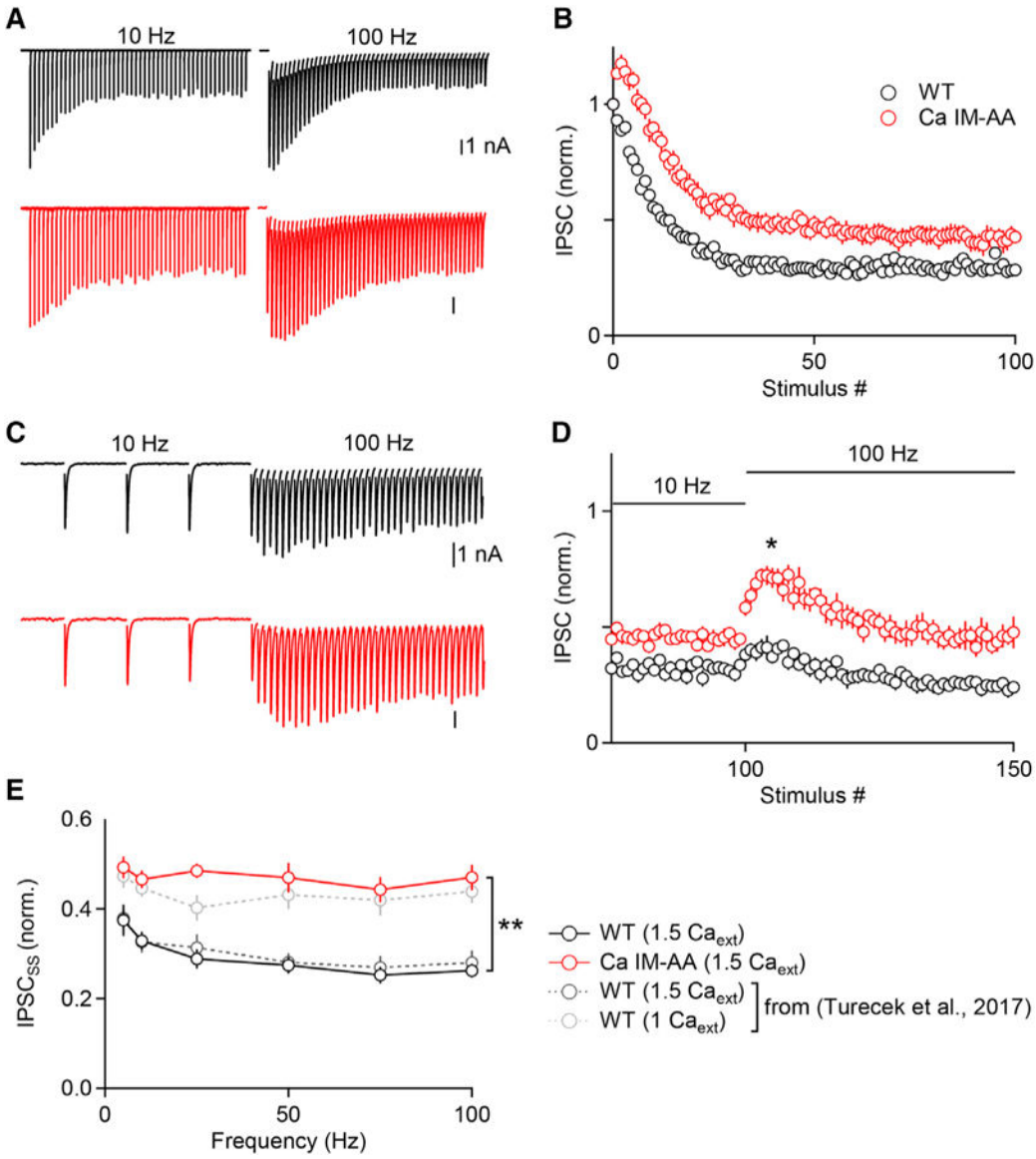

Figure 3. Elimination of $Ca_V2.1$ Channel Facilitation Paradoxically Increases Train Facilitation at the PC-DCN Synapse

PC axons were stimulated with stimulus trains and the resulting inhibitory postsynaptic currents (IPSCs) were recorded from DCN neurons for WT (black) and Ca IM-AA (red) mice.

(A) Representative IPSCs evoked by10 Hz and 100-Hz trains are shown.

(B) Summary of normalized IPSC amplitudes evoked by 10-Hz stimulation.

(C) Synaptic currents are shown for 10 Hz stimulation followed by 100-Hz stimulation.

(D) Summary of IPSC amplitudes evoked by an abrupt increase from 10-to 100-Hz stimulation. Statistical significance (unpaired Student's t test; see Table S1): *$p < 0.05$.

(E) Normalized average steady-state IPSC amplitudes ($IPSC_{SS}$) are plotted for 5-to 150-Hz stimulation. Dashed lines indicate summaries from previous studies (Turecek et al., 2017) for WT animals at different levels of external calcium (Ca_{ext}). 100 Hz $IPSC_{SS}$ significantly

different between WT and Ca IM-AA animals (**$p < 0.01$; unpaired Student's t test; see Table S1).

Data are shown as mean ± SEM.

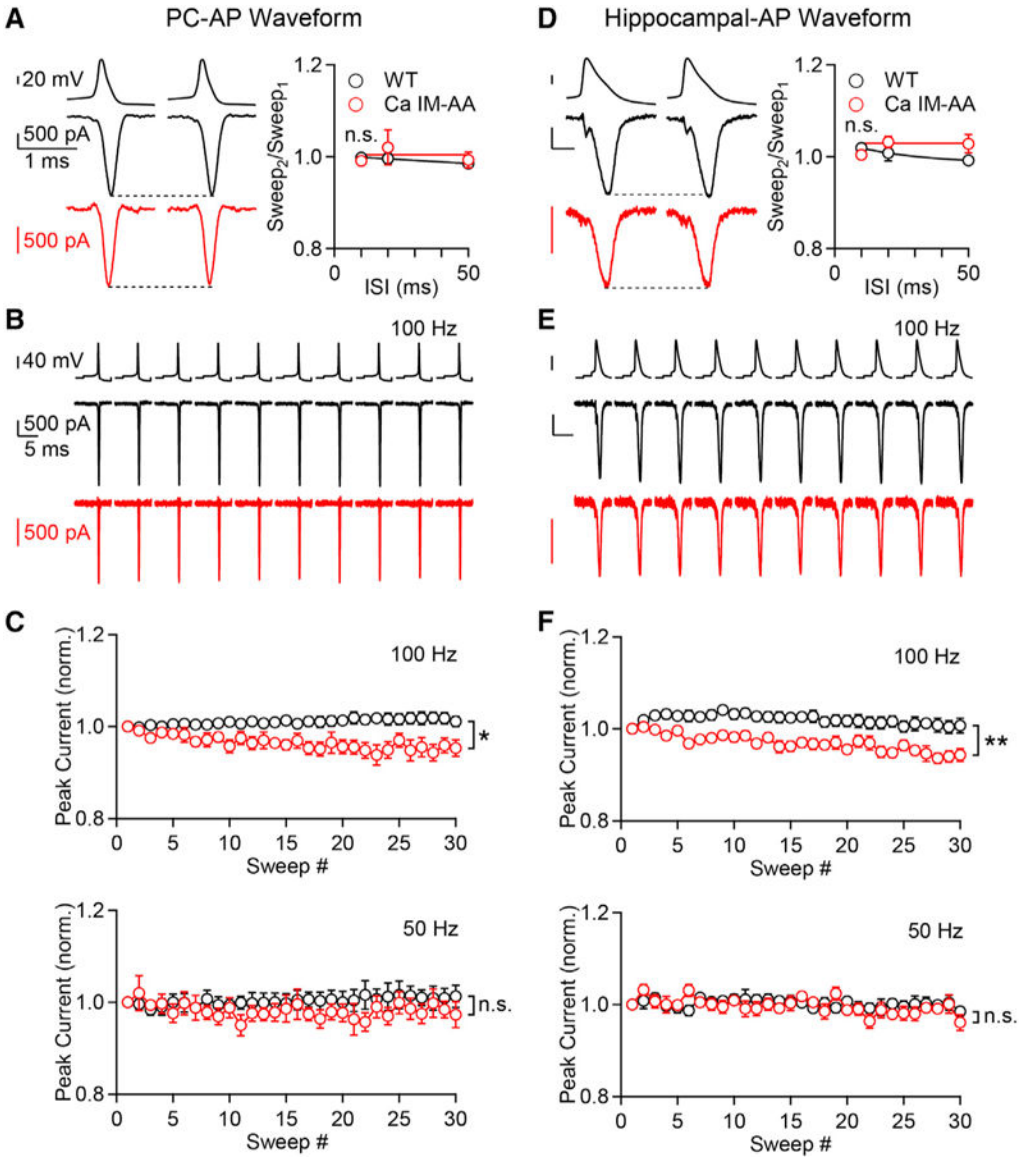

Figure 4. $Ca_V2.1$ Channel Facilitation Is Small in Physiological Ca_{ext} at Physiological Temperatures

Experiments were performed in acutely dissociated Purkinje cells (PCs) at 37°C with 1.5 mM Ca_{ext}. Calcium currents were evoked by trains of action potential (AP) waveforms from cerebellar PCs (PC; left) and hippocampal pyramidal cells (right).

(A and D) Left: currents evoked by representative PC (A) and hippocampal (D) AP waveforms are shown for wild-type (black) and Ca IM-AA (red) mice. The same scale values were used for (A) and (D). Right: summary of the ratio of calcium current evoked by second and first stimuli plotted for different inter-sweep intervals (ISIs) and AP wave-forms (data from trains in C and F), with each sweep corresponding to an AP waveform stimulus.

(B and E) Representative PC (B) and CA1 (E) AP waveforms and PC responses for the first ten sweeps of a 100-Hz train. The same scale values were used for (B) and (E).

(C and F) Normalized peak calcium current evoked by different frequency trains plotted versus the sweep number, with each sweep corresponding to an AP waveform stimulus, for PC-AP waveform (C) and hippocampal-AP waveform (F).

Statistical significance (unpaired Student's t test; see Table S1): *$p < 0.05$; **$p < 0.01$, not significant (n.s.). Data are shown as mean ± SEM.

KEY RESOURCES TABLE

REAGENT or RESOURCE	SOURCE	IDENTIFIER
Chemicals, Peptides, and Recombinant Proteins		
NBQX disodium salt	Abcam	Cat# ab120046
(R,S)-CPP	Abcam	Cat# ab120160
SR95531 (Gabazine)	Abcam	Cat# ab120042
AM251	Abcam	Cat# ab120088
Picrotoxin	Abcam	Cat# ab120315
Strychnine HCl	Sigma Aldrich	Cat# S-8753
CGP 55845 hydrochloride	Abcam	Cat# ab120337
QX-314 Chloride	Abcam	Cat# ab120118
Tetrodotoxin with citrate	Alomone	Cat# T-550
w-Conotoxin GVIA	Sigma Aldrich	Cat# C9915
Nimodipine	Sigma Aldrich	Cat# N149
TTA-A2	Alomone	Cat# T-140
Experimental Models: Organisms/Strains		
Ca IM-AA Mouse	Ingenious Targeting Laboratory	see (Nanou et al., 2016b, 2016a)
Software and Algorithms		
Igor Pro 6	Wavemetrics	https://www.wavemetrics.com
MultiClamp 700B Commander	Molecular Devices / Axon Instruments	https://www.moleculardevices.com
MafPC	Courtesy of M. A. Xu-Friedman	https://www.xufriedman.org/mafpc
MATLAB	Mathworks	https://www.mathworks.com/products/matlab.html
Adobe Illustrator	Adobe	https://www.adobe.com/products/illustrator.html
GraphPad Prism 7	GraphPad Software, Inc.	https://www.graphpad.com
Microsoft Excel	Microsoft	https://products.office.com/en-us/excel